Supporting Information to:

Brownmillerite-type Ca_2FeCoO_5 as a Practicable Oxygen Evolution Reaction Catalyst

Etsushi Tsuji,[*ab] Teruki Motohashi,[**ac] Hiroyuki Noda,[d] Yoshitaka Aoki,[ad]
Damian Kowalski,[a] Hajime Tanida,[e] Junji Niikura,[e] Yukinori Koyama,[e]
Masahiro Mori,[e] Hajime Arai,[e] Tsutomu Ioroi,[f] Naoko Fujiwara,[f]
Yoshiharu Uchimoto,[g] Zempachi Ogumi [e] and Hiroki Habazaki [ad]

[a] *Division of Applied Chemistry, Faculty of Engineering, Hokkaido University, Sapporo, Japan*

[b] *Department of Chemistry and Biotechnology, Graduate School of Engineering, Tottori University, Tottori, Japan*

[c] *Department of Materials and Life Chemistry, Kanagawa University, Yokohama, Japan*

[d] *Graduate School of Chemical Sciences and Engineering, Hokkaido University, Sapporo, Japan*

[e] *Office of Society-Academia Collaboration for Innovation, Kyoto University, Kyoto, Japan*

[f] *National Institute of Advanced Industrial Science and Technology (AIST), Osaka, Japan*

[g] *Graduate School of Human and Environmental Studies, Kyoto University, Kyoto, Japan*

CONTENTS

*e-mail: e-tsuji@chem.tottori-u.ac.jp. **e-mail: t-mot@kanagawa-u.ac.jp.

Experimental Section

Synthesis. For CFCO_S1100, a stoichiometric mixture of $CaCO_3$ (Wako Pure Chemical, 99.99%), Fe_2O_3 (Wako Pure Chemical, 99.9%) and Co_3O_4 (Rare Metallic Co. Ltd., 99.9%) was fired in air at 1100 °C for 24 h. For syntheses of $Ca_2Fe_{2-x}Co_xO_5$_W600/W800, $LaFe_{0.5}Co_{0.5}O_3$ (LFCO) and BSCF, the following reagents were used as starting materials: $Ca(NO_3)_2{\cdot}4H_2O$ (Kanto Chemical, 99.9%), $La(NO_3)_3{\cdot}6H_2O$ (Kanto Chemical, 99.9%), $Ba(NO_3)_2$ (Wako Pure Chemical, 99.9%), $Sr(NO_3)_2$ (Kanto Chemical, 99.9%), $Fe(NO_3)_3{\cdot}9H_2O$ (Kanto Chemical, 99.9%) and $Co(NO_3)_2{\cdot}6H_2O$ (99.9%, Wako Pure Chemical). Appropriate amounts of these reagents were dissolved in Milli-Q water in which an equal molar of citric acid (Wako Pure Chemical, 98%) was subsequently added as a complex agent. The citrate solution was stirred and heated at 60 – 70 °C to promote polymerization. The gelatinous product was prefired in air at 450 °C for 1 h and then fired at 600 °C, 800 °C ($Ca_2Fe_{2-x}Co_xO_5$) or 1000 °C (LFCO and BSCF) for 12 h. The RuO_2 powder (99.9%) was used as purchased from Sigma-Aldrich.

Characterization. Phase purity of the catalysts was checked by means of X-ray powder diffraction (XRD; Rigaku, Ultima IV) using Cu Kα radiation. The grain morphology of each catalyst was observed using a scanning electron microscope (SEM; JEOL JSM-6500F) operated at 10 kV. In order to estimate the surface areas of the catalysts, nitrogen gas adsorption/desorption isotherms (Bel Japan, Belsorp-max instrument) were measured at 77 K. The X-ray absorption near edge structure (XANES) measurements were performed at the beamline BL28XU of SPring-8 (Hyogo, Japan).[S1] The synchrotron radiation X-ray from the storage ring was monochromated with a Si 111 double-crystal monochromator. The XANES spectra were measured in the transmission mode using two ionization chambers. Data reduction was carried out with the Demeter software package.[S2] The electrical conductivity was measured for the $Ca_2Fe_{2-x}Co_xO_5$ samples employing a four-point-probe method with a powder resistivity measurement system (Mitsubishi Chemical Analytech, MCP-PD51). Approximately 1 g of each powder sample was put into a cylindrical measurement cell equipped with four electrodes at the bottom of the cell. The powder was compressed with a piston at the given pressure and then the conductivity was measured as a function of the loaded pressure. Oxygen nonstoichiometry of CFCO was investigated by means of thermogravimetry (TG; Rigaku, TG8120). The measurement was carried out for a 40 mg specimen under O_2 and N_2 atmospheres in a temperature range of 50 ~ 800 °C with

a scan rate of 10 °C min^{-1}.

Density functional theory calculations. Density functional theory (DFT) calculations were performed using the plane-wave basis projector augmented wave method implemented in VASP code.[S3] Energies of $Ca_2Fe_{2-x}Co_xO_5$ (x = 0, 0.25, 0.50 0.75 and 1.0) were calculated for all possible arrangements of iron/cobalt ions within the unit cell composed of four formula units. The plane-wave basis set was determined with a cutoff energy of 500 eV. The exchange correlation interaction was treated by the generalized gradient approximation with the Hubbard model correction (GGA+U).[S4,S5] The effective U parameters of 5 eV were used for both iron and cobalt. Spin polarization was considered assuming parallel magnetic structures. Integral in the reciprocal space was evaluated by the Gaussian smearing technique with a smearing parameter of 0.1 eV and a 4×1×4 mesh. Atomic positions and lattice constants were optimized until the residual forces and stress became smaller than 0.01 eV $Å^{-1}$ and 0.05 GPa, respectively.

Electrochemical measurements for OER activity. Working electrodes for the OER measurements were prepared as follows. 50 mg of the catalyst, 10 mg of acetylene black (AB) treated by nitric acid, and 60 mg of 5 wt% Na^+-exchanged Nafion solution were dispersed ultrasonically in 5 mL of ethanol to obtain a homogenous black suspension. The AB additive was obtained by immersing a commercial AB powder into concentrated nitric acid at 80 °C overnight, then filtering and drying at 100 °C overnight. The Na^+-exchanged Nafion solution was obtained by mixing a 5 wt% Nafion solution (Wako Pure Chemical) with an appropriate amount of 0.1 mol dm^{-3} NaOH ethanol solution. Then, 20 μL of the suspension was pipetted onto the surface of a 5-mm-diameter glassy carbon (GC) electrode with a rotation rate of 500 rpm.

The electrochemical measurements were carried out utilizing a potentiostat (Hokuto Denko, HZ-7000) combined with a rotating disk electrode (RDE; Pine Instrument Co., AFMSRCE). A platinum sheet and an Hg/HgO/KOH electrode were used as a counter and a reference electrode, respectively; the working electrode was GC-RDE loaded with 1.0 mg cm^{-2} of the catalyst at a rotation rate of 1600 rpm. All the measurements were conducted at room temperature (~25 °C) in a 4 mol dm^{-3} KOH aqueous solution (pH 14) saturated with oxygen (99.5%). It should be emphasized that the usage of concentrated alkaline solutions is mandatory for constructing practical metal-air secondary batteries to enhance the ionic conductivity of the electrolyte and to suppress corrosions of the negative electrodes. Such OER data with high KOH concentrations are thus informative to evaluate the performance in practical metal-air secondary batteries. The potential U

was converted from the Hg/HgO reference scale to the RHE using the following equation.

$$U \text{ vs RHE} = U \text{ vs Hg/HgO} + 0.098 + 0.059 \times \text{pH}$$

In each measurement, the potential of the catalyst-loaded GC-RDE was swept from 1.10 V to 1.70 V vs RHE with a potential sweep rate of 1 mV s^{-1}. Prior to the potential sweep, the surface of the catalyst was pretreated by applying 30 potential cycles between 1.3 and 0.6 V vs. RHE with a sweep rate of 50 mV s^{-1}. For all the measurements, the current density has been *iR*-corrected with a solution resistance (R = 3.2 Ω).

Cyclic durability test. The electrode used for the cyclic durability test consisted of a gas-diffusion layer (GDL) and an active layer. The hydrophobic GDL was prepared from a mixture of 70 wt% graphitized carbon black (TOKAI CARBON, #3855) and 30 wt% of PTFE (dispersant). The resultant carbon/PTFE mixture was rolled in several steps to thin sheets. The active layer was formed by pulse-spraying a catalyst ink onto the thin sheet to obtain an electrode surface loaded with CFCO_W600 of 8.5 mg cm^{-2}. To prepare the catalyst ink, CFCO_W600 and graphitized carbon black were ultrasonically dispersed in water containing a surfactant (5% in concentration) for 25 min, then PTFE (dispersant) was added and blended for 3 min. The final composition of the active layer was: CFCO/carbon/PTFE = 53/27/20 in wt%. After drying the catalyst ink at 60 °C for 30 min, the electrode assembly was heated at 350 °C in flowing argon gas for 13 min to impregnate the PTFE and to remove the surfactant. The assembly was cut out to form a 1.5 cm square and a nickel mesh (60 mesh) current collector was pressed on the top of GDL.

The OER/ORR cyclic durability test was conducted in a 4 mol dm^{-3} KOH aqueous solution at room temperature (24 ± 2 °C). The test cell made of acrylic resin was equipped with a working electrode (gas-diffusion electrode with a geometric surface area of 1.0 cm^2), a nickel plate counter electrode, and an Hg/HgO/KOH reference electrode. The gas-diffusion electrode was exposed to ambient air without forced flow, see the photograph in Fig. 4a. A galvanostat (Biologic, VMP300) was employed to apply a constant current of 20 mA cm^{-2} while the potential of the working electrode was measured. A single OER/ORR cycle includes ORR for 1 h, open circuit for 3 min, OER for 1 h, and open circuit for 3 min. Prior to the OER/ORR cycles, the electrode was conditioned by potential sweeps between 0.42 V and 1.67 V vs. RHE with a potential sweep rate of 1 mV s^{-1} for ten times. The potential values are shown on a reversible hydrogen electrode (RHE) basis without ohmic loss corrections.

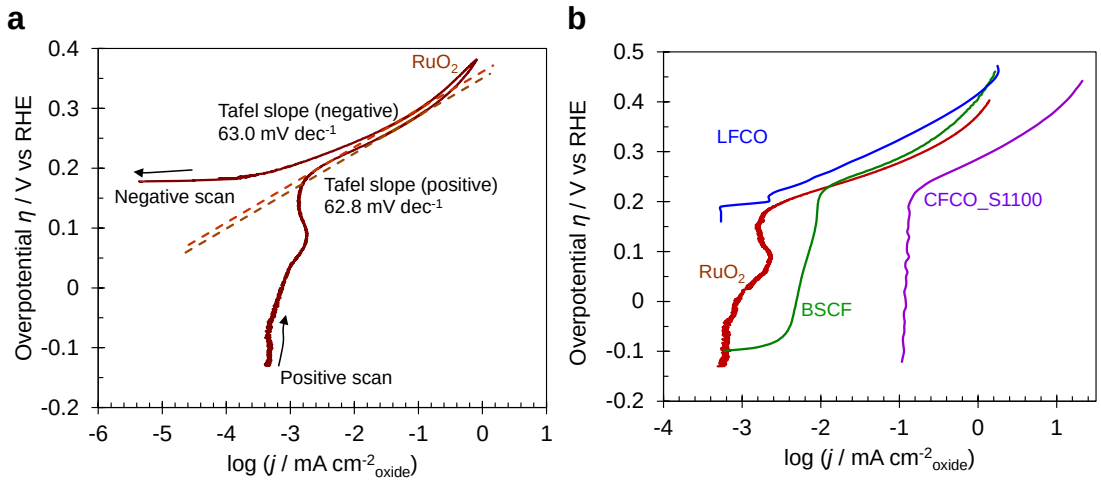

Figure S1. (a) Log *j* vs overpotential curve of RuO_2 measured by cyclic voltammetry, and (b) those of CFCO_S1100, LFCO, BSCF and RuO_2 measured by linear sweep voltammetry in a 4 M KOH aqueous solution in a potential range of 1.2 – 1.65 V vs RHE.

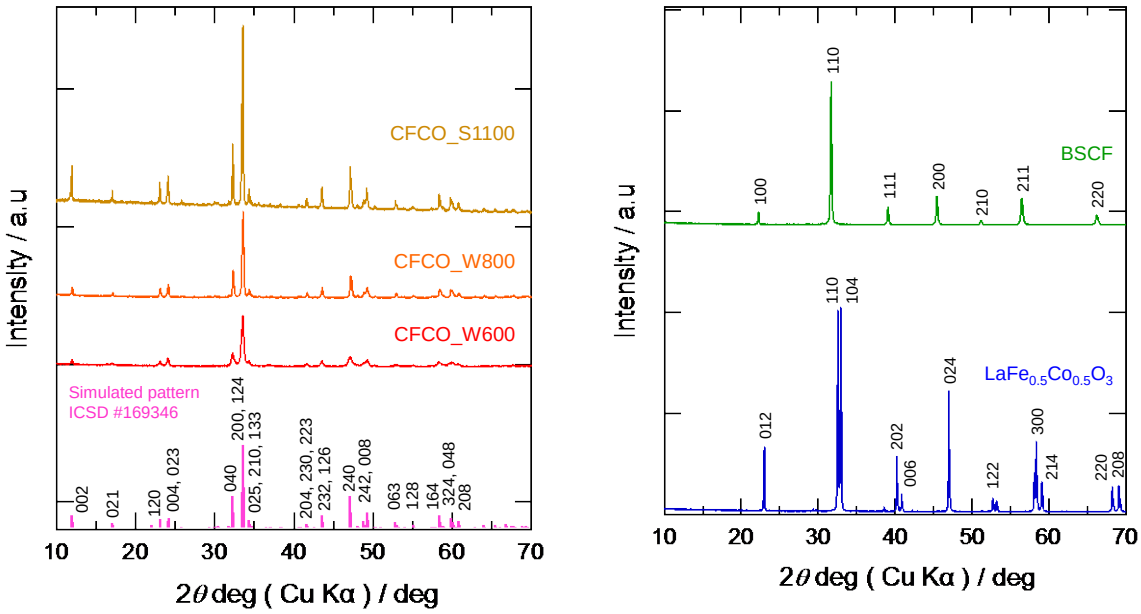

Figure S2. (a) XRD patterns for the CFCO_S1100, W800 and W600 samples. The pattern for the precursor powder via a wet-chemical route is also presented. For the S1100 sample, diffraction lines are indexed on the basis of the brownmillerite (BM)-type structural model (orthorhombic *Pbcm*) reported in the literature.[36] Note that *hkl* indices for strong diffraction lines are only shown. (b) XRD patterns for BSCF and LFCO. The patterns for these oxides are readily indexed on the basis of the perovskite-type structural models (cubic *Pm*-3*m* and rhombohedral *R*-3*c*, respectively).

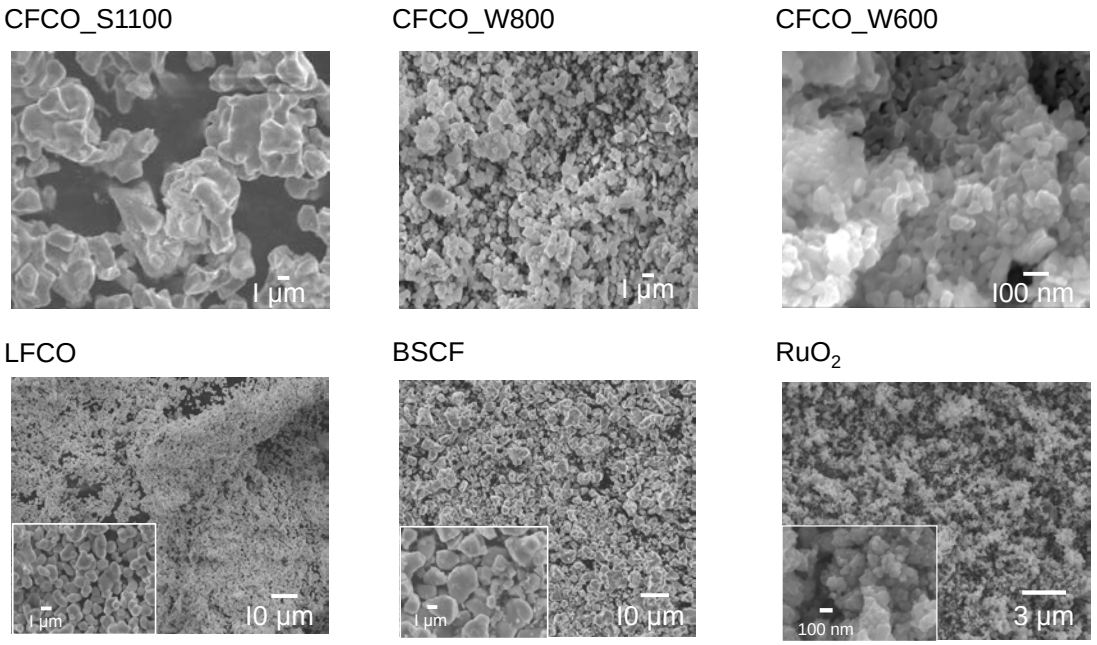

Figure S3. Scanning electron micrographs of CFCO and reference catalysts. SEM images of the CFCO_S1100, W800 and W600, LFCO, BSCF and RuO_2 powders.

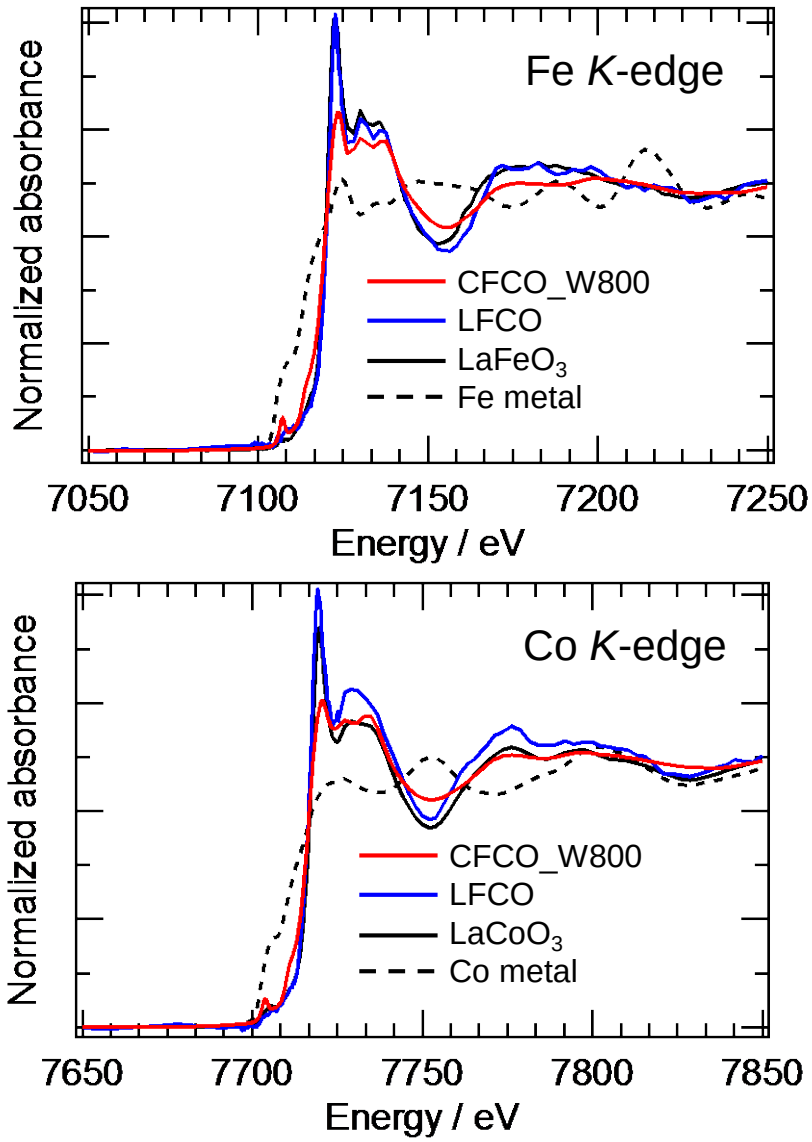

Figure S4. Iron and cobalt *K*-edge XANES spectra. The absorption edge energies in the spectra are correlated to the oxidation states of iron and cobalt. The absorption edge energies of iron and cobalt in CFCO_W800, LFCO, and $LaFeO_3$ are larger than those of metallic iron and cobalt. The iron and cobalt species in these oxides are most likely trivalent.

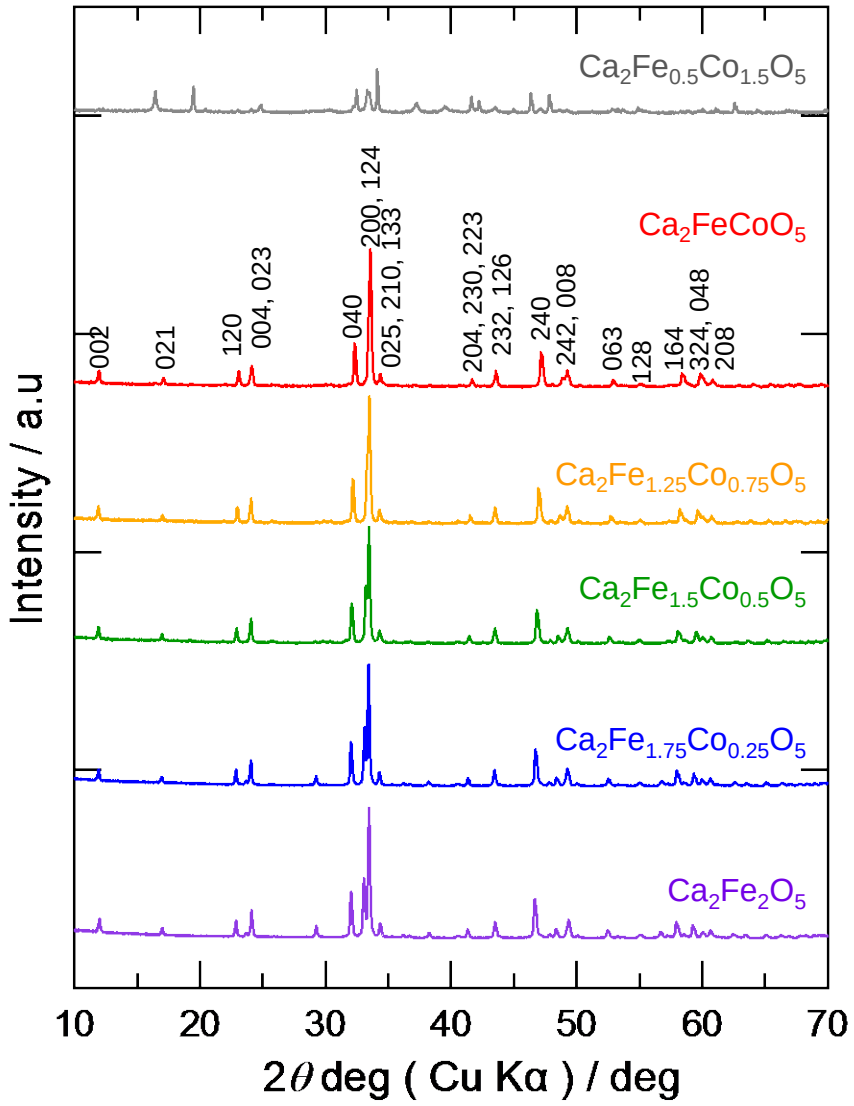

Figure S5. X-ray diffraction patterns for $Ca_2Fe_{2-x}Co_xO_5$ ($0 \leq x \leq 1.5$). The x = 0, 0.25, 0.50, 0.75, 1.0 samples are phase pure of the $Ca_2Fe_{2-x}Co_xO_5$ solid solution with a BM structure (note that *hkl* indices for strong diffraction lines are only shown). The synthesis of BM-type $Ca_2Fe_{0.5}Co_{1.5}O_5$ (x = 1.5) was unsuccessful.

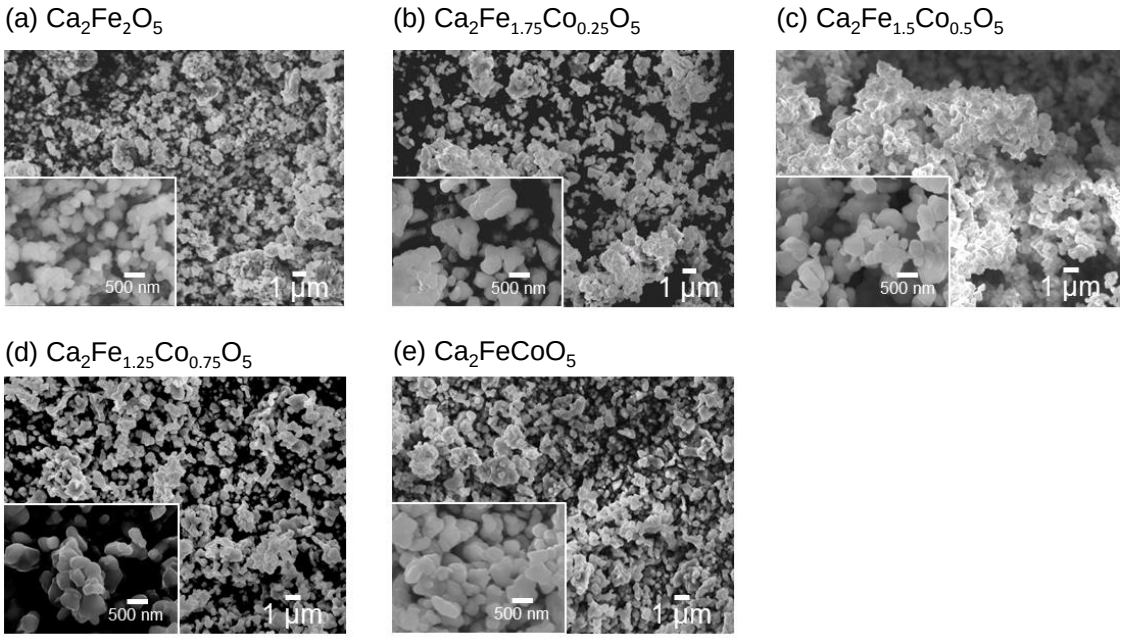

Figure S6. Scanning electron micrographs of $Ca_2Fe_{2-x}Co_xO_5$ ($0 \leq x \leq 1$). SEM images of the phase-pure $Ca_2Fe_{2-x}Co_xO_5$ samples with x = 0, 0.25, 0.50, 0.75 and 1.0.

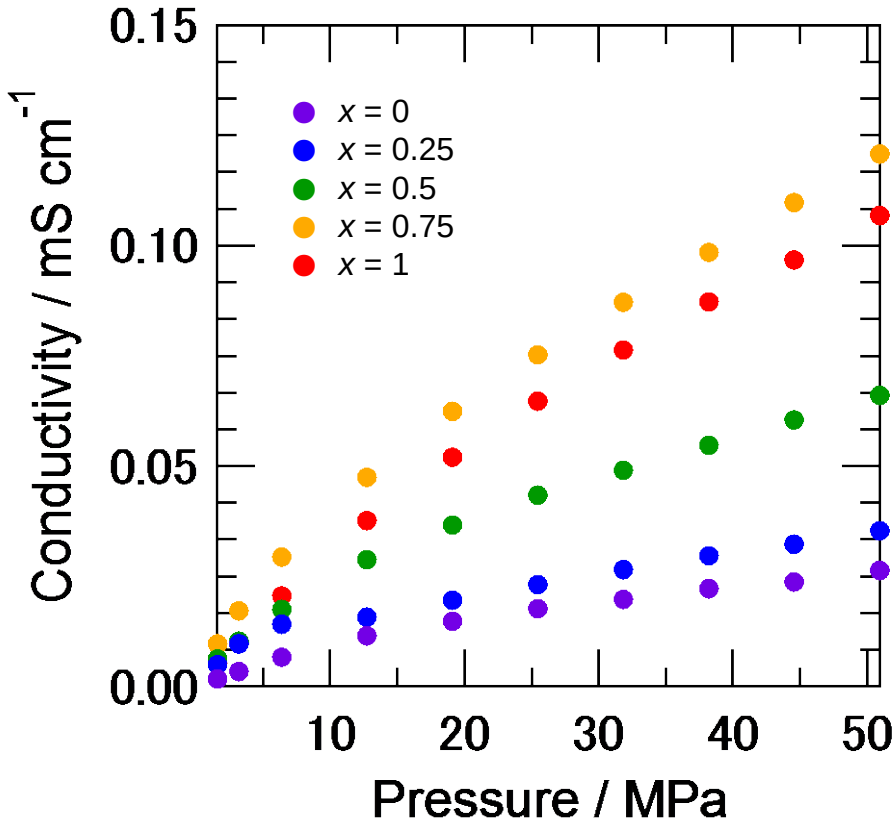

Figure S7. Electrical conductivity of $Ca_2Fe_{2-x}Co_xO_5$ ($0 \leq x \leq 1$). Electrical conductivity of the uniaxially-compressed powders of $Ca_2Fe_{2-x}Co_xO_5$ as a function of the loaded pressure.

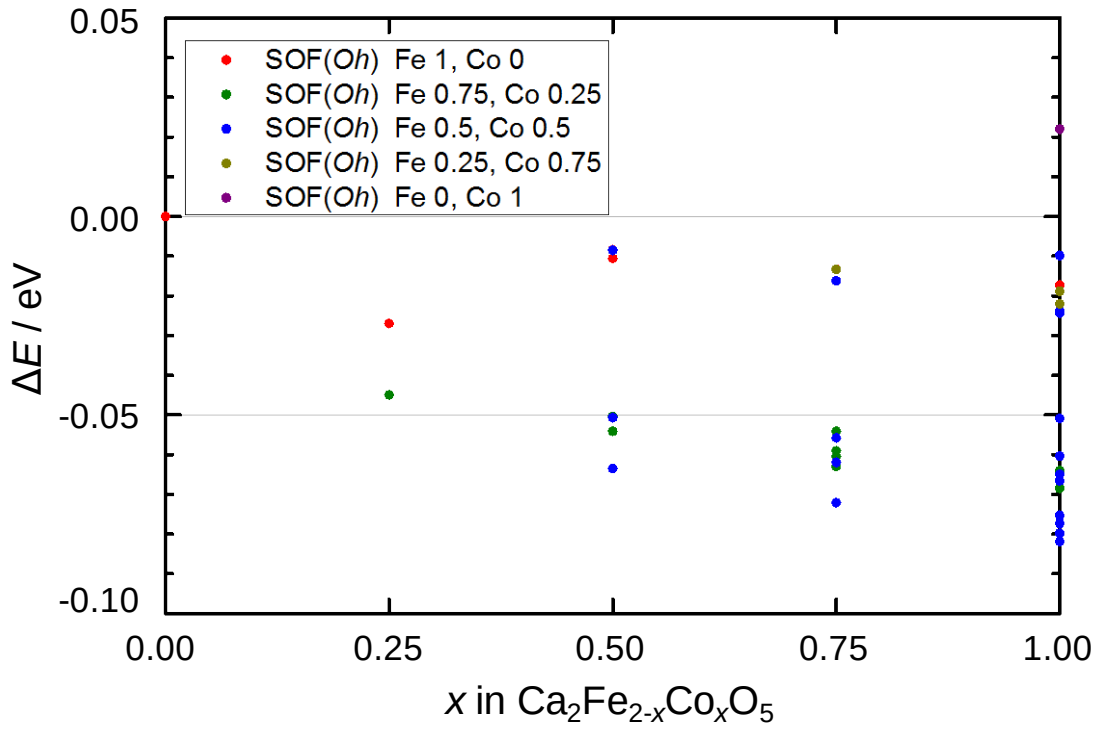

Figure S8. Energy of $Ca_2Fe_{2-x}Co_xO_5$ ($0 \leq x \leq 1$) with respect to the BM-type $Ca_2Fe_2O_5$ and $Ca_2Co_2O_5$ evaluated by DFT calculations. Each point denotes an individual atomic arrangement of iron and cobalt ions within the unit cell. The arrangements are categorized by site occupation fraction (SOF) of the *Oh*-coordinated site.

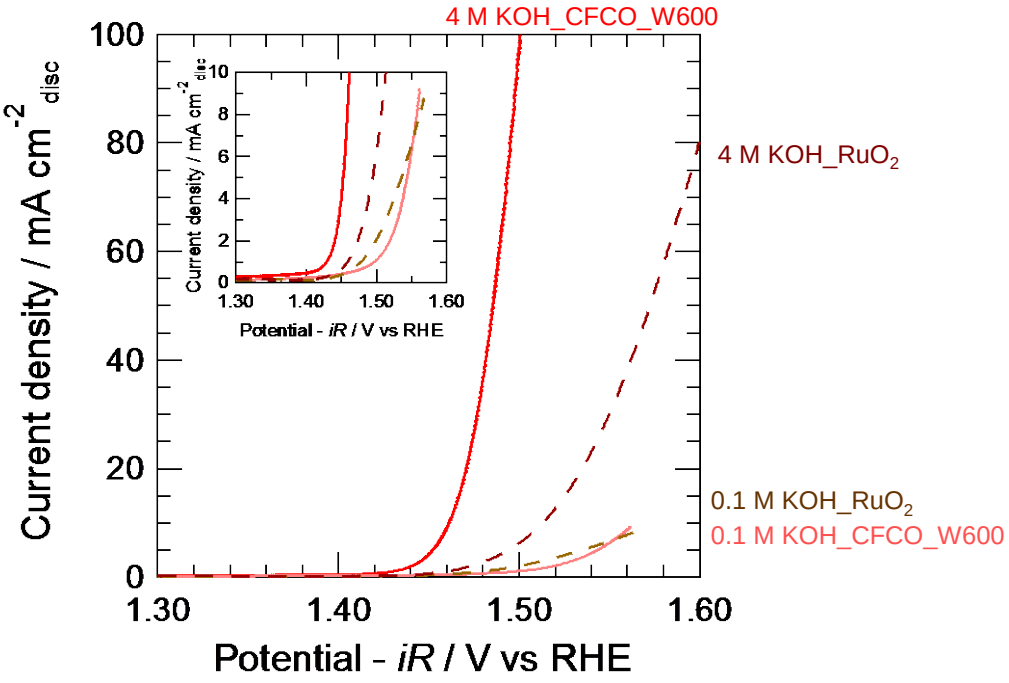

Figure S9. Linear sweep voltammograms of CFCO_ W600 and RuO_2 in 0.1 and 4 mol dm^{-3} KOH aqueous solutions. The current density was normalized with the geometric surface area of the disc electrode. It should be noted that the overpotential of CFCO_W600 decreased with increasing the concentration of hydroxide anions in the electrolyte, whereas that of RuO_2 was almost constant.

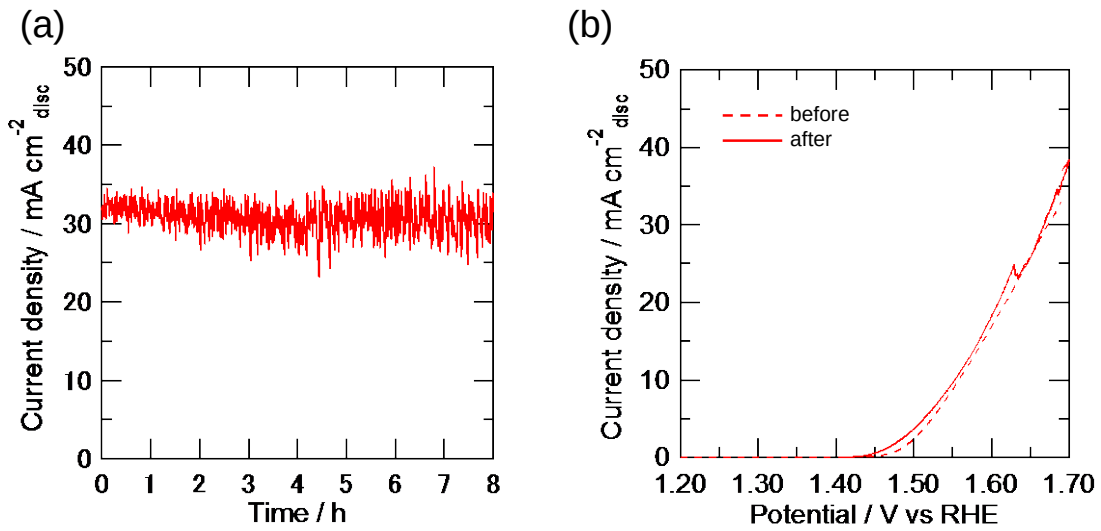

Figure S10. (a) Current density vs time plot with an applied constant potential of 1.7 V vs RHE. The current density is nearly constant during the OER test for 8 h. (b) Linear sweep voltammograms before and after the application of the constant potential, demonstrating that the OER activity is essentially identical. In the OER test, a catalyst ink containing the CFCO_W800 powder alone (without acetylene black (AB) as a conductive additive) was dropped on the graphite-sheet electrode to avoid extrinsic variations in the OER current caused by the decomposition of AB. The as-prepared working electrode was not pretreated by 30 CV cycles. The current density in this measurement was much smaller than that presented in Fig. 2 because of the absence of the conductive additive.

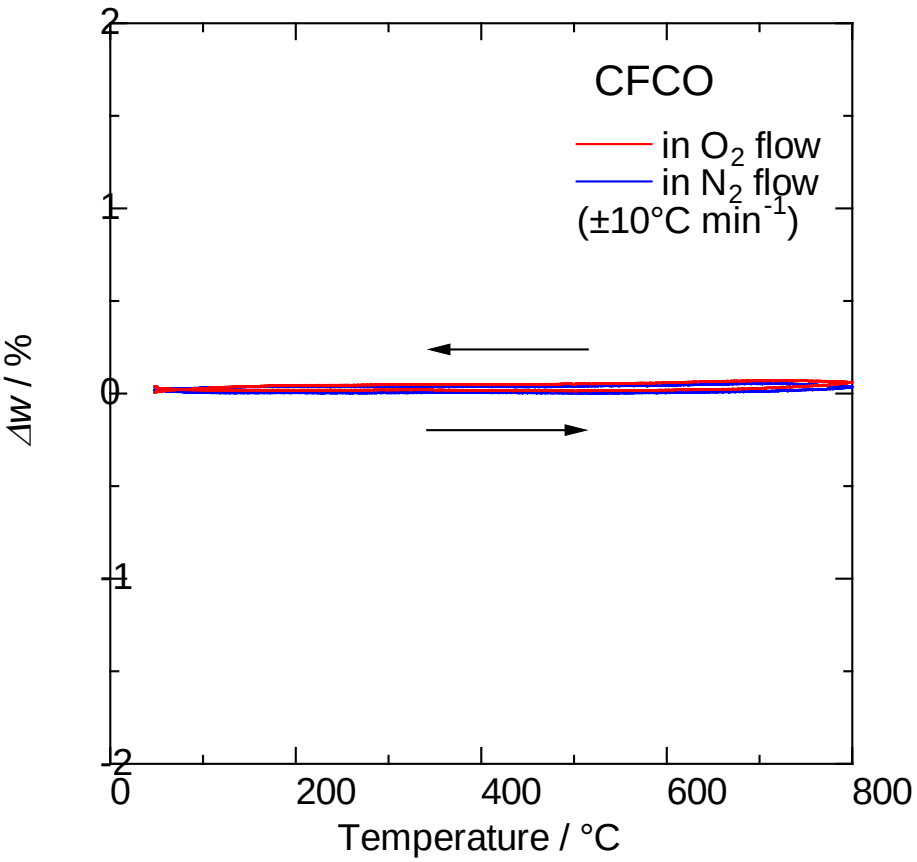

Figure S11. TG data of CFCO. Thermogravimetric (TG) curves measured under O_2 and N_2 atmospheres. The data were acquired in a temperature range of 50 ~ 800 °C with heating/cooling rates of ±10 °C min^{-1}.

Table S1. Specific surface areas of CFCO and reference catalysts.

Samples	BET surface area / m^2 g^{-1}
CFCO_S1100	0.134
CFCO_W800	2.86
CFCO_W600	18.9
LFCO	0.725
BSCF	0.669
RuO_2	8.38

Table S2. Specific surface areas of the $Ca_2Fe_{2-x}Co_xO_5$ samples ($0 \leq x \leq 1$).

Samples	BET surface area / m^2 g^{-1}
$Ca_2Fe_2O_5$	2.66
$Ca_2Fe_{1.75}Co_{0.25}O_5$	2.63
$Ca_2Fe_{1.5}Co_{0.5}O_5$	2.31
$Ca_2Fe_{1.25}Co_{0.75}O_5$	2.66
Ca_2FeCoO_5 (CFCO)	2.86

Table S3. Amount of dissolution of CFCO_W800 after the OER test for 8 h. The condition of the OER test was the same as Supplementary Fig. 8.

Element	Ca	Fe	Co
Amount of dissolution / wt%	0.45	DL	DL

DL: below the detection limit

REFERENCES

[S1] H. Tanida, K. Fukuda, H. Murayama, Y. Orikasa, H. Arai, Y. Uchimoto, E. Matsubara, T. Uruga, K. Takeshita, S. Takahashi, M. Sano, H. Aoyagi, A. Watanabe, N. Nariyama, H. Ohashi, H. Yumoto, T. Koyama, Y. Senba, T. Takeuchi, Y. Furukawa, T. Ohota, T. Matsushita, Y. Ishizawa, T. Kudo, H. Kimura, H. Yamazaki, T. Tanaka, T. Bizen, T. Seike, S. Goto, H. Ohno, M. Takata, H. Kitamura, T. Ishikawa, T. Ohta, Z. Ogumi, *J. Synchrotron Rad.* **2014**, *21*, 268-272.

[S2] B. Ravel, M. Newville, *J. Synchrotron Rad.* **2005**, *12*, 537-541.

[S3] G. Kresse, J. Furthmüller, *Phys. Rev. B* **1996,** *54*, 11169–11186.

[S4] J. P. Perdew, K. Burke, M. Ernzerhof, *Phys. Rev. Lett.* **1996**, *77*, 3865–3868.

[S5] S. L. Dudarev, G. A. Botton, S. Y. Savrasov, C. J. Humphreys, A. P. Sutton, *Phys. Rev. B* **1998**, *57*1505–1509.